The Evidence For Electrical Currents in Cosmic Plasma

ANTHONY L. PERATT, SENIOR MEMBER, IEEE

Abstract—**With the advent of fully three-dimensional, fully electromagnetic, particle-in-cell simulations, investigations of Birkeland currents and magnetic-field-aligned electric fields have become possible in plasmas not accessible to *in situ* measurement; i.e., in plasmas having the dimensions of galaxies or systems of galaxies.**

The importance of applying electromagnetism and plasma physics to the problem of radiogalaxy and galaxy formation derives from the fact that the universe is largely matter in its plasma state; i.e., a *plasma universe*. The motion of this plasma across weak magnetic fields can lead to the generation of electromotive forces, the energy of which can be transported over large distances via Birkeland currents. The dissipation of this energy in localized regions can lead to pinches and condensed states of matter. Where double layers form in the pinches, strong electric fields can accelerate the charged particles to high energies.

The necessity for a three-dimensional electromagnetic approach derives from the fact that the evolution of magnetized plasmas involves complex geometries, intense self-fields, nonlinearities, and explicit time-dependence.

The observational evidence for galactic-dimensioned Birkeland currents is given based on the comparison of the synchrotron radiation properties of simulated currents to those of extra-galactic sources.

I. Introduction

An electromotive force $\int \boldsymbol{v} \times \boldsymbol{B} \cdot d\boldsymbol{s}$ giving rise to electrical currents in conducting media is produced wherever a relative perpendicular motion of plasma and magnetic fields exists [1], [2]. An example of this is the (nightside) sunward-directed magnetospheric plasma that cuts the earth's dipole field lines near the equatorial plane, thereby producing a potential supply that drives currents within the auroral circuit.

A. Birkeland Currents

The tendency for charged particles to follow magnetic lines of force and therefore produce field-aligned currents has resulted in the widespread use of the term "Birkeland currents" in space plasma physics [3]. Their discovery in the Earth's magnetosphere in 1974 has resulted in a drastic change in our understanding of aurora dynamics, now attributed to the filamentation of Birkeland charged-particle sheets following the Earth's dipole magnetic-field lines into vortex current bundles. The importance of Birkeland currents in astrophysical settings has been stressed by Fälthammar [4].

Laboratory analogs to the magnetospheric Birkeland currents and a tabulation of possible occurrences of Birkeland currents in astrophysical plasmas, with dimensions ranging from 10^2 to nearly 10^{21} m, and currents of 10^5 to 10^{19} A, have been given [5].

B. Field-Aligned Electric Fields

Recent literature in the area of magnetospheric physics reflects considerable interest in magnetic-field-aligned electric fields. Such electric fields can have important consequences in cosmic plasma [6], including the "unfreezing" of magnetic fields, the acceleration of electrons to very high energies, and filamentation of the plasma itself.

In magnetized nonhomogeneous astrophysical plasma, a number of mechanisms are present that can generate field-aligned electric fields. These include anomolous resistivity caused by wave–particle interactions, collisionless thermoelectric effects due to energy-dependent wave-particle interactions, magnetic mirror effects involving trapped particles in magnetic-field gradients, and electric double layers due to localized charge separation. While all of the above mechanisms have been studied in the laboratory and simulated by computer, it is the last mechanism that has been found to be remarkably prolific in producing appreciable potential drops in neutral plasma. Moreover, Birkeland currents and double layers appear to be associated phenomena, and both laboratory experiments [7] and computer simulations [8] have shown the formation of a series of double layers along current-carrying plasma filaments or beams.

When double layers (or a series of double layers) form in adjacent Birkeland current filaments, field-aligned electric fields are generated, which then serve to accelerate electrons and ions within these regions.

II. Filamentary Currents in the Plasma Universe

A. Galactic Dimensioned Birkeland Currents

By extrapolating the size and strength of magnetospheric currents to galaxies, Alfvén [9] suggests a number of confined-current regions that flow through interstellar clouds and assist in their formation. For example, a galactic magnetic field of the order $B_G = 10^{-9}$–10^{-10} T associated with a galactic dimensions of 10^{20}–10^{21} m suggests that the galactic current be of the order $I_G = 10^{17}$–

Manuscript received June 1, 1989. This work was supported by the U.S. Department of Energy.

The author is with the Los Alamos National Laboratory, MS-B259, Los Alamos, NM 87545.

IEEE Log Number 8933497.

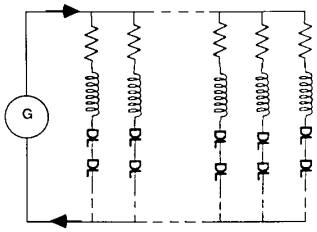

Fig. 1. Electrical equivalent circuit of the plasma universe. Each filament of plasma is represented by a resistance, inductance, and a series of double layers in which particle beams are accelerated to high energies.

10^{19} A. As a natural extension of the size hierarchy in cosmic plasmas, the existence of galactic-dimensioned Birkeland currents or filaments has been hypothesized [5], [11], [12].

In the galactic-dimensioned Birkeland current model, the width of a typical filament may be taken to be 35 kpc ($\sim 10^{21}$ m), separated from neighboring filaments by a similar distance. Since current filaments in laboratory plasmas generally have a width/length ratio in the range 10^{-3} to 10^{-5}, a typical 35 kpc wide filament may have an overall length between 35 Mpc and 3.5 Gpc, with an average length of 350 Mpc.

Fig. 1 is an electrical equivalent circuit of the metagalaxy (plasma universe) consisting of a large number of filaments with resistance R, inductance L, and sustaining a series of double layers in each of the filaments.

B. The Large-Scale Structure of the Plasma Universe

Surface currents, delineating plasma regions of different magnetization, temperature, density, and chemical composition give space a cellular structure [12]. As current-carrying sheet beams collect into filaments, the morphology of the surface currents is filamentary.

For the case of tenuous cosmic plasmas the thermokinetic pressure is often negligible, and hence the magnetic field is force-free. Under the influence of the electromagnetic fields the charged particles drift with the velocity

$$\boldsymbol{v} = (\boldsymbol{E} \times \boldsymbol{B})/B^2. \tag{1}$$

The overall plasma flow is inwards and matter is accumulated in the filaments which, because of their qualitative field-line pattern, are called "magnetic ropes" [12]. Magnetic ropes should therefore tend to coincide with material filaments that have a higher density than the surroundings. The cosmic magnetic ropes or current filaments are not observable themselves, but the associated filaments of condensed matter can be observed by the radiation they emit and absorb.

It is because of the convection and neutralization of plasma into radiatively cooled current filaments (due to synchrotron losses) that matter in the plasma universe should often display a filamentary morphology. For this reason, quasars and galaxies must form within the filamented sheets of cosmic plasma.

Table I tabulates the basic physical characteristics of the plasma universe.

TABLE I
BASIC PROPERTIES OF THE PLASMA UNIVERSE

item	The Plasma Universe
Geometry	Euclidean Flat, infinite
Structure	Cellular/Filamentary, all scales
Age	Infinite
Principle molding force	Electromagnetism/Gravitation
Origin of detected radiation	
radio	discrete sources
microwave	discrete sources
optical	discrete sources
X-rays	discrete sources
γ-rays	discrete sources
Origin of the elements	All elements formed in Pre-Metagalactic epoque, continuing synthesis of elements in stars.
Red Shifts	Metagalactic expansion (not more than 90%) matter-antimatter anihilation, plasma convection into filaments, plasma and optical effects.
Quasars, Radio Galaxies	Filamental disruptions (double layers).
Cosmic Rays	Charged particle acceleration in double layers.
'Missing Mass'	Electromagnetic forces.

TABLE II
SIMULATION DERIVED PARAMETERS FOR THE DOUBLE RADIO GALAXY CYGNUS A

parameter	simulation value
Galactic current, I_z, A	$2{\cdot}15 \times 10^{19}$
Galactic magnetic field, G	$2{\cdot}5 \times 10^{-4}(B_0)$
	$2{\cdot}0 \times 10^{-4}(B_{z0})$
Plasma temperature, keV	2·0–32·0
Plasma density, n_e, cm^{-3}	$1{\cdot}79 \times 10^{-3}$
Electric field strength, E_{z0}, mV/m	62
Power emitted in synchrotron radiation, W	$1{\cdot}16 \times 10^{37}$
Radiation burst duration, s	$1{\cdot}28 \times 10^{14}$
Age since contraction initiation, s	$5{\cdot}76 \times 10^{14}$
Total energy delivered to source, ergs	$6{\cdot}3 \times 10^{62}$

III. THE BIOT–SAVART FORCE IN COSMICAL ELECTRICAL NETWORKS

A. Long-Range R^{-1} Attraction

Because of the emf-induced current I_z, a galactic filament can be expected to maintain its columnar, filamental form provided that the Bennett-pinch condition is satisfied; i.e., that

$$I_z^2 > 8\pi NkT/\mu_0 \tag{2}$$

where $T = T_e + T_i$.

In addition to confining plasma in filaments radially, the axial current flow produces another important effect: A long-range interactive force on other galactic filaments. Fig. 2 illustrates the geometry under analysis. The Biot–Savart electromagnetic force between filaments is

$$\boldsymbol{F}_{21} = \int \boldsymbol{j}_2 \times \boldsymbol{B}_{21} d^3r \tag{3}$$

for all space, where $\boldsymbol{j} \times \boldsymbol{B}$ is the Lorentz force. Since the current path greatly exceeds the filament widths, the attractive force between two similarly oriented filaments is

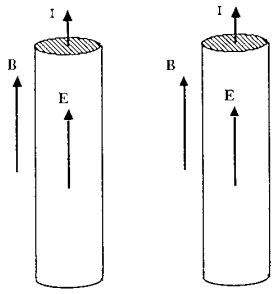

Fig. 2. Basic geometry under analysis: Two parallel Birkeland currents formed by the tendency of charged particles to follow magnetic lines of force $\boldsymbol{B}$ and to pinch due to their own induced magnetic field. Because of the magnetic-field-aligned electric field $\boldsymbol{E}$, each filament is a double layer.

approximately given by

$$\boldsymbol{F}_{21}(I_{z1}, I_{z2}) = -\hat{\boldsymbol{r}}\,\frac{\mu_0 I_{z1} I_{z2}}{2\pi R} \tag{4}$$

where the subscripts 1 and 2 denote columns 1 and 2, respectively, and R is their separation.

B. Short-Range R^{-3} Repulsion

Because of the axial magnetic field B_z, the particles spiral as they drift or accelerate and thereby produce an azimuthal component in the generalized current $\boldsymbol{I} = \hat{z}I_z + \hat{\theta}I_\theta$. The force between the azimuthal currents I_θ is

$$\boldsymbol{F}_{21}(I_{\theta 1}, I_{\theta 2}) = \frac{\mu_0 \pi a}{4\pi R^3} I_{\theta 1} I_{\theta 2}(\hat{\boldsymbol{r}} \sin\theta - \hat{\theta} 2 \cos\theta), \qquad R \gg a \tag{5}$$

where $\hat{r}$ and $\hat{\theta}$ are the (cylindrical coordinate) unit vectors, and a is the radius of an azimuthal current.

Hence the electromagnetic forces between filaments are ordered as R^{-1} (long-range attractive) and R^{-3} (short-range repulsive). At coalescion distances, the total force is somewhat more complicated than that described by (4) and (5). Fig. 3 depicts the character of the interaction force as a function of separation distance and shows a map of B_θ produced by the superposition of induced magnetic fields from each filament.

C. Electromagnetic Torque

The inward velocity v of each filament produced by (4) generates a $\boldsymbol{v} \times \boldsymbol{B}$ force in the x-y plane of the cross sections of the filaments in Fig. 2. The electrons in the left-hand filament are displaced in the $+y$ direction, while those in the right-hand filament are displaced in the $-y$ direction. As a consequence of this displacement, the axial electric currents carried by the electrons are displaced towards the $\pm y$ direction surfaces. This polarization displacement of currents imparts a net clockwise torque on the filaments, causing them to spiral together.

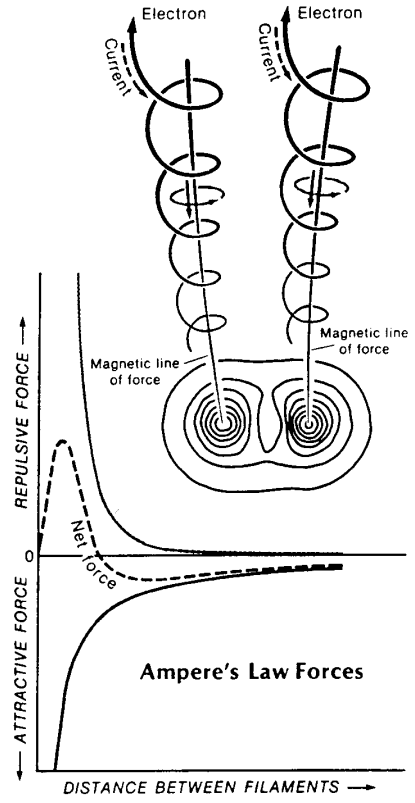

Fig. 3. The forces between two adjacent Birkeland currents: that is, electric currents aligned along magnetic field lines. The parallel components of current (dark gray lines) are long-range attractive, while the counter-parallel azimuthal currents (light gray rings) are short-range repulsive. A third force, long-range electrostatic repulsion, is found if the electrons and ions are not present in equal numbers. These forces cause the currents to form sheets, filaments or "magnetic ropes," and they can be found far from the source region. A projection of the current-induced magnetic fields is shown above the graph.

IV. Synchrotron Emission from Pinched Particle Beams

One of the most important processes that limit the energies attainable in particle accelerators is the radiative loss by electrons accelerated by the magnetic field of a betatron or synchrotron. This mechanism was first brought to the attention of astronomers by Alfvén and Herlofson in 1950 [13]; a remarkable suggestion at a time when plasma, magnetic fields, and laboratory physics were thought to have little, if anything, to do with a cosmos filled with "island" universes (galaxies). Synchrotron radiation is characterized by a generation of frequencies appreciably higher than the cyclotron frequency of the electrons; a continuous spectra (for a population of electrons) whose intensity decreases with frequency beyond a critical frequency (near intensity maxima); increasing beam directivity with increasing $\gamma(\gamma = (1 - \beta^2)^{-1/2})$; and polarized electromagnetic wave vectors.

A. Synchrotron Emitting Z-Pinches

Charged particle beams held together or pinched by their self-magnetic fields have been of general interest since their earliest investigation by Bennett [14]. The macroscopic picture of such a beam is that of a self-consistent magnetic confinement or compression against the expansion due to thermal pressure (equation (2)). On the microscopic scale, the individual particle orbits include radial oscillations due to the Lorentz force superimposed on the drift in the direction of mean flow. Since they imply particle acceleration, there is electromagnetic radiation associated with them. Because the force is a $\boldsymbol{v} \times \boldsymbol{B}$ force, the radiation from the relativistic electrons is synchrotron radiation.

Manifestations of the pinch effect appear for a laboratory observer as a rapidly occurring phenomena. A burst of radiation from high-current discharges (with current densities of the order $10^{11}\mathrm{A/cm^2}$), such as low-inductance vacuum sparks, plasma focus devices, and exploded wires, is found over a broad spectral range; from the microwave region to the hard X-ray region. Recorded data show that the radiation bursts are correlated with dips in the current waveform. The microwave radiation observed is attributed to synchrotron radiation of electrons in the magnetic field of the pinch current. The hard X-ray quanta are attributed to synchrotron radiation from the electrons at the transitions between Landau levels in this same current-induced magnetic field. Theoretical treatments of synchrotron radiation from Z-pinches have been given by Meierovich [15] and Newberger *et al.* [16].

B. Radiation Directivity

The radiation gain from electrons undergoing helical trajectories, such as in Z-pinches, has been derived by Johner [17]. The mean power emitted per electron per solid angle Ω in the direction of observation $\boldsymbol{n}$ is

$$\frac{dP(\theta)}{d\Omega} = \frac{e^2\omega_b^2}{32\pi^3\epsilon_0 c}(1-\beta^2)\beta_\perp^2 F(\beta_\parallel, \beta_\perp, \theta) \quad (6)$$

where

$$F(\beta_\parallel, \beta_\perp, \theta) = \frac{4g_\parallel^2\left[(1-\beta_\parallel^2)(1-\cos^2\theta) - 4\beta_\parallel\cos\theta\right] - (1-\beta_\parallel^2+3\beta_\perp^2)\beta_\perp^2\sin^4\theta}{4(g_\parallel^2-\beta_\perp^2\sin^2\theta)^{7/2}} \quad (7)$$

and $g_\parallel(\theta) = 1 - \beta_\parallel\cos\theta$, where θ is the angle between $\boldsymbol{B}_0$ and $\boldsymbol{n}$.

In a way analogous to the directivity of an antenna, the gain $G(\theta)$ is defined as

$$G(\theta) = \frac{dP(\theta)/d\Omega}{P^T_{\mathrm{circular}}/4\pi} \quad (8)$$

where we have chosen to normalize to the total circular power radiated by an electron

$$P^T_{\mathrm{circular}} = \frac{e^2\omega_b^2}{6\pi\epsilon_0 c}\frac{\beta_\perp^2}{1-\beta^2} \quad (9)$$

where

$$\omega_b = eB_0/m_e.$$

From (6)–(9),

$$G(\beta_\parallel, \beta_\perp, \theta) = \tfrac{3}{4}(1-\beta^2)^2 F(\beta_\parallel, \beta_\perp, \theta). \quad (10)$$

Equation (10) is plotted in polar coordinates in Fig. 4 for a variety of helical pitch-angle cases. Whereas the principal direction of radiation for an electron rotating about a magnetic field is the plane of rotation, the radiation from an electron with a large parallel velocity component (as compared to the perpendicular velocity) is along $\boldsymbol{B}_0$.

C. Synchrotron Bursts of Microwaves from Simulations

An enhancement of radiated power is achieved when the sum of the $\boldsymbol{v} \times \boldsymbol{B}$ radial forces seen by the relativistic electrons (equation (3)) is increased, as is the case when the azimuthal magnetic fields of neighboring pinches are present (Fig. 3). While no theoretical treatment of synchrotron enhancement from beam interactions is known, this phenomena has been examined in some detail, both experimentally and with simulations. Whenever the attractive force between simulation columns causes their separation to be reduced to a distance such that the repulsive force (equation (5)) starts to become comparable to the attractive force (equation (4)), a burst in the radiation occurs (Fig. 5). For the parameters used in these simulations, this distance is of the order of several pinch radii. As shown in Fig. 5, the radiation from the kiloelectronvolt particles is polarized in the transverse plane, and the synchrotron enhancement (burst) is detected in the x and y electric radiation energies ($W_{\mathrm{ER}x}$, $W_{\mathrm{ER}y}$) *and the* z magnetic radiation energy ($W_{\mathrm{BR}z}$). The burst lasts until the induced axial magnetostatic energy W_{Bz}, due to the azimuthal current I_θ, is depleted (because the counterparallel azimuthal current force (equation (5)) brakes the azimuthal electron flow in both filaments). For some simulational parameters, W_{Bz} can build-up and discharge again in the form of additional bursts of synchrotron radiation. The longtime slowly varying increase in radiation in $W_{\mathrm{ER}x}$ *and* $W_{\mathrm{ER}y}$ is due to the buildup of electrostatic energy from charge separation in the particle number and size-constrained simulation model. The cell size and timestep parameters used in the simulations are $\Delta' = 1.66 \times 10^{20}$ m and $dt' = 5.87 \times 10^{11}$ s.

D. Total Power Emitted

An estimate of the total power emitted as synchrotron radiation follows directly from the simulations. During

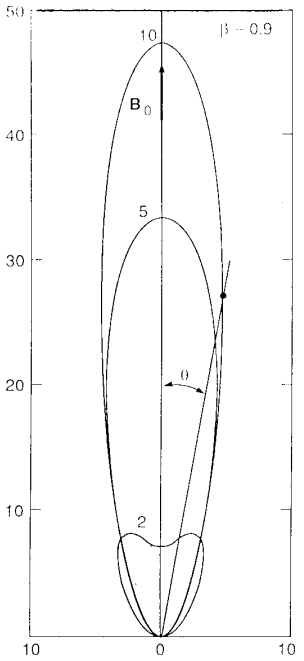

Fig. 4. Gain pattern for $\beta = 0.9$. The curves shown are for $\beta_\parallel/\beta_\perp = 2$, 5, and 10.

the radiation "burst era" at $T = 90$, the total energy radiated in the form of electric- and magnetic-field energy is $W_{\text{rad}} = 2.1$ AEU, while the total simulation magnetostatic energy is $W_{\text{ms}} = 350$ AEU. Since, at $T = 90$, $B_z = 2.0 \times 10^{-8}$ T, $B_\theta = 2.5 \times 10^{-8}$ T, and $V \sim 10^{63}$ m^3 is the plasma volume; $W_{\text{ms}} = (2\mu_0)^{-1} B^2 V = 2.5 \times 10^{53}$ J, or 1 AEU $= 7.1 \times 10^{50}$ J. The peak radiation burst lasts $\sim 20\ dt'$ in the compressed time frame (Fig. 5), corresponding to an actual time of $20(6 \times 10^{11}\ \text{s})\sqrt{(1836/16)} = 1.28 \times 10^{14}$ s. The total power emitted in synchrotron radiation is $L = 2.1 \times 7.1 \times 10^{50}\ \text{J}/1.28 \times 10^{14}\ \text{s} = 1.16 \times 10^{37}$ W (Table II).

E. Isophotal Patterns

The isophotal contours of the synchrotron emission can be determined by plotting the magnetic- and electric-field energies from which the radiation derives. These are shown in Fig. 6 as a function of time, spanning 10.7 to 58.7 Myr after the start of filament interaction. Initially, the current is uniformly distributed over the pinch, but, after a few Myr, the most intense current flow occurs at the outer boundary of each filament. This is a consequence of the growing strength of the repulsive force. The current cross section at the outer filament boundary takes on a "C" or cusp-shape within which a very intense cross section of current, or "spot," is located. These spots are juxtapositioned in opposing filaments and mark the beginning of a rotation of filaments brought about by a polarization field in each filament (Section III-C). The hot spots are, of course, the most intense radiators of synchrotron radiation along $\boldsymbol{B}_0$.

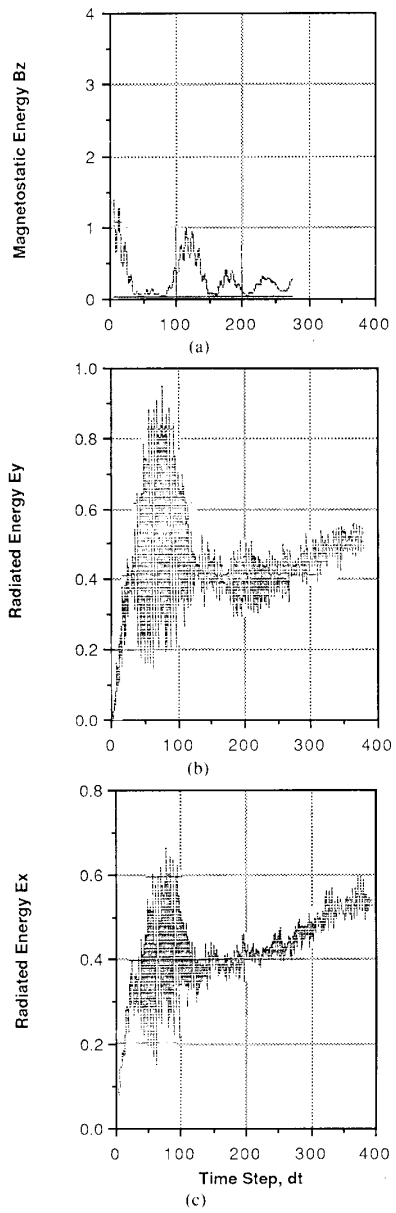

Fig. 5. (a) Self-consistent axially directed magnetic field energy versus time. (b) and (c) Energy lost via synchrotron radiation in the x and y electric field components, respectively. The ordinate is in arbitrary energy units of $7.1 \times 10^{50}\ j$, while the abscissa is in simulation time units $dt' = 6 \times 10^{11}\ s$.

Frame by frame, the hot-spot "cusps" move inward with time as the rotation continues. The actual radiation patterns are determined by both the magnetic and electric energy distributions as plotted in Fig. 6. At very late time in the evolution of the radiating source, ~ 60 Myr, the radiation isophotes take on "butterfly"-like patterns that finally extinguish as the synchrotron burst-era comes to an end in the embryo stage of the development of a galaxy.

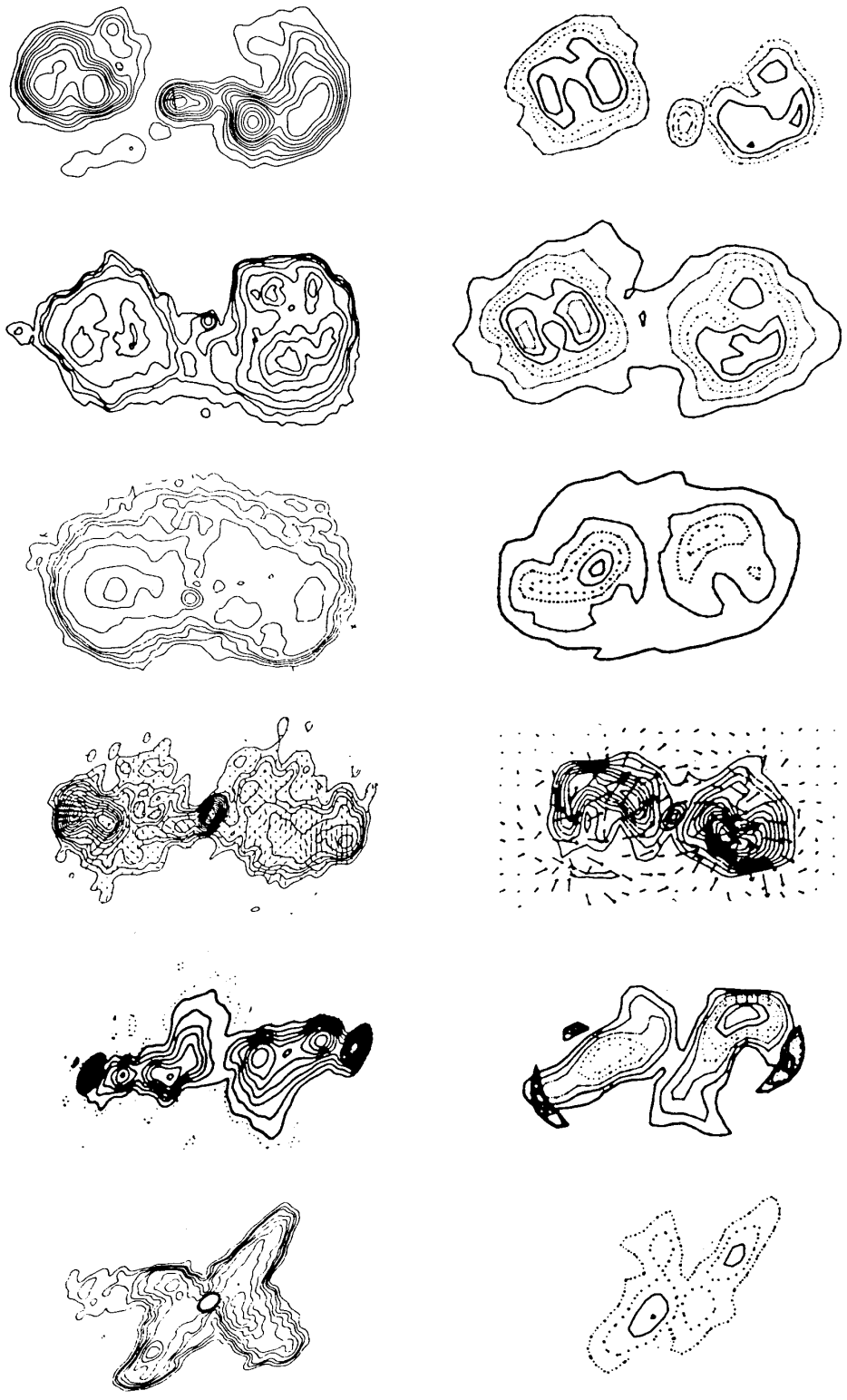

(a) (b)

Fig. 6. (a) Synchrotron isophotes (various frequencies) of the double radio sources 0844 + 319, Fornax A, 3C310, 2355 + 490, 3C192, and 3C315. (b) Simulation analogs at times 10.4 Myr to 58.7 Myr. Time increases from top to bottom.

F. Comparison to Radio Galaxies

The monochromatic power of quasars and double radio galaxies span a range of about 10^{33} to 10^{39} W [11]. For example, the "prototype" double radio galaxy Cygnus A has an estimated radio luminosity of $1.6\text{–}4.4 \times 10^{37}$ W. Together with the power calculated in Section IV-D, the simulation isophotes are very close to those observed from this object [5]. Fig. 6(a) suggests that, apparently, double radio galaxies previously held unrelated all belong to the same species, but are simply seen at different times in their evolution.

V. Conclusions

With the advent of three-dimensional electromagnetic particle-in-cell simulations, investigations of Birkeland currents have become possible in plasmas not accessible to *in situ* measurement; i.e., in plasmas having the dimensions of galaxies or systems of galaxies. The necessity for a three-dimensional electromagnetic approach derives from the fact that the evolution of magnetized plasmas involves complex geometries, intense self-fields, nonlinearities, and explicit time-dependence. Moreover, synchrotron radiation and double layers are discrete particle phenomena and cannot be studied using magnetofluid models of plasma. The importance of applying electromagnetism and plasma physics to the problem of radio galaxy, galaxy, and star formation derives from the fact that the universe is largely matter in its plasma state; i.e., a *plasma universe*. The motion of this plasma in local regions can lead to pinches and can ultimately condense states of matter. Where double layers form, strong electric fields can accelerate particles to high energies. The intensity and patterns of synchrotron radiation observed in the model simulations are in excellent agreement with those observed from double radio galaxies.

Lastly, this paper has treated the special case of the radiation seen by an observer when the observer happens to be located in the directed pattern of a synchrotron source. Many sources with this orientation can be expected in various regions of the sky from the "spaghetti" of radiating filaments surrounding the viewer. The background spectrum caused by an extremely large number of synchrotron radiating filaments, when the observer is not in the directed beam, is treated in a separate paper [18].

The problem regarding the large redshifts of quasars has not been addressed in this paper. However, it is noteworthy that the geometry depicted in Fig. 2 is identical to that used by Bocko *et al.* to demonstrate a redshift in the directed beam via the Wolf effect [19].

References

[1] H. Alfvén, "Double layers and circuits in astrophysics," *IEEE Trans. Plasma Sci.*, vol. PS-14, pp. 779–793, 1986.

[2] S.-I. Akasofu, "The magnetospheric currents: An introduction to magnetospheric currents," in *Magnetospheric Currents* (Geophys. Monograph No. 28), T. A. Potemra, Ed. Washington, DC: Amer. Geophys. Union, 1984, pp. 29–48.

[3] A. J. Dessler, "Evolution of arguments regarding existence of field aligned currents," in *Magnetospheric Currents* (Geophysical Monograph No. 28) T. A. Potemra, Ed. Washington, DC: Amer. Geophys. Union, 1984.

[4] C.-G. Fälthammar, "Magnetosphere–ionosphere interactions—near-earth manifestations of the plasma universe," *IEEE Trans. Plasma Sci.*, vol. PS-14, pp. 616–628, 1986.

[5] A. L. Peratt, "Evolution of the plasma universe: I. Double radio galaxies, quasars, and extragalactic jets," *IEEE Trans. Plasma Sci.*, vol. PS-14, pp. 639–660, 1986.

[6] C.-G. Fälthammar, "Magnetic-field aligned electric fields," *ESA J.*, vol. 7, pp. 385–401, 1983.

[7] C. Chan and N. Hershkowitz, "Transistion from single to multiple double layers," *Phys. Fluids*, vol. 25, pp. 2135–2137, 1982.

[8] A. L. Peratt and M. E. Jones, "Particle-in-cell simulations of heavy ion double layers," presented at the IEEE Conf. Record, Saskatoon, Can., 1986.

[9] H. Alfvén, "Electric currents in cosmic plasma," *Rev. Geophys. and Space Sci.*, vol. 15, pp. 271–284, 1977.

[10] A. L. Peratt and J. C. Green, "On the evolution of interacting magnetized galactic plasmas," *Astrophys. Space Sci.*, vol. 91, pp. 19–33, 1983.

[11] A. L. Peratt, "Evolution of the plasma universe: II. The formation of systems of galaxies," *IEEE Trans. Plasma Sci.*, vol. PS-14, pp. 763–778, 1986.

[12] H. Alfvén and C.-G. Fälthammar, *Cosmical Electrodynamics*. Oxford, Eng.: Oxford Univ. Press, 1963.

[13] H. Alfvén and N. Herlofson, "Cosmic radiation and radio stars," *Phys. Rev.*, vol. 78, p. 616, 1950.

[14] W. H. Bennett, "Magnetically self-focusing streams," *Phys. Rev.*, vol. 45, pp. 890–897, 1934.

[15] B. E. Meierovich, "Electromagnetic collapse, problems of stability, emission of radiation and evolution of a dense pinch," *Phys. Rep.*, vol. 104, pp. 259–347, 1984.

[16] B. S. Newberger, M. I. Buchwald, R. R. Karl, D. C. Moir, and T. P. Starke, "Synchrotron radiation from Bennett beams," *Bull. Amer. Phys. Soc.*, vol. 29, p. 1435, 1984.

[17] J. Johner, "Angular distribution of the total cyclotron radiation of a relativistic particle with parallel velocity," *Phys. Rev. A*, vol. 36, pp. 1498–1501, 1988.

[18] W. Peter and A. L. Peratt, "Synchrotron radiation spectrum for galactic-sized plasma filaments," *IEEE Trans. Plasma Sci.*, this issue, pp. 49–55.

[19] M. F. Bocko, D. H. Douglass, and R. S. Knox, "Observation of frequency shifts of spectral lines due to source correlations," *Phys. Rev. Lett.*, vol. 58, pp. 2649–2651, 1987.

*

Anthony L. Peratt (S'60–M'63–SM'85) was born in Belleville, KS, in 1940. He received the B.S.E.E. degree from California State Polytechnic University, Pomona, in 1963, the M.S.E.E. degree from the University of Southern California, Los Angeles, in 1967, and the Ph.D. degree in electrical engineering in 1971, also from the University of Southern California.

He was with the Aerospace Corp., Satellite Communications Group, and from 1972 to 1979 was a Staff Member at the Lawrence Livermore National Laboratory. He served as a Guest Scientist at the Max Planck Institute for Plasma Physics, Garching (1975–1977), and at the Department of Plasma Physics, The Royal Institute of Technology, Stockholm (1985). Since 1981 he has been with the Applied Theoretical Physics Division of the Los Alamos National Laboratory, Los Alamos, NM. His research interests have included wave coupling in nonuniform plasmas, diagnosis of plasmas with laser light and plasma holography, laser–plasma interaction theory, z pinches, and the particle-in-cell simulation of pulsed-power generators, magnetically insulated transmission lines, double layers, and microwave and synchrotron radiation from laboratory and astrophysical sources.

Dr. Peratt was Guest Editor of the IEEE TRANSACTIONS ON PLASMA SCIENCE Special Issue on Space and Cosmic Plasma (December 1986, April 1989); Guest Editor, *Laser and Particle Beams* Special Issue on Particle Beams and Basic Phenomena in the Plasma Universe (August 1988); and Session Organizer for Space Plasmas, IEEE International Conferences on Plasma Science, 1987–1989. He was elected to the IEEE Nuclear and Plasma Sciences Society ExCom, and holds membership in the American Physical Society, the American Astronomical Society, and Eta Kappa Nu.